

## Nestlike Hollow Hierarchical MCM-22 Microspheres: Synthesis and Exceptional Catalytic Properties

Naibo Chu, Jinqu Wang, Yan Zhang, Jianhua Yang,\* Jinming Lu, and Dehong Yin

State Key Laboratory of Fine Chemicals, Institute of Adsorption and Inorganic Membrane, School of Chemical Engineering, Dalian University of Technology, 158 Zhongshan Road, Dalian 116012, China

Received December 2, 2009. Revised Manuscript Received March 11, 2010

The synthesis and exceptional catalytic performance of nestlike hollow hierarchical MCM-22 microspheres (MCM-22-HS) were presented. The MCM-22-HSs were obtained by one-pot rotating hydrothermal synthesis using carbon black as a hard template via self-assembly combined hydrothermal crystallization. The shell of MCM-22-HS was hierarchically constructed by many flaky MCM-22 crystals. The Mo/MCM-22-HS exhibited significantly improved methane conversion, yield of benzene product and catalyst lifetime for methane dehydroaromatization as a model reaction. The exceptional catalytic performance was attributed to the hollow and hierarchical structure. Faster transfer of Mo species because of the existing mesopores and higher dispersion of Mo species brought by the higher external surface of the Mo/HMCM-22-HS lead to generation of more catalysis active sites and high benzene yield. The sites associated with catalyst deactivation could also be reduced, contributing to improvement of the catalyst lifetime. Both the hierarchical and hollow structure is favorable for the diffusion of larger molecule product, probably contributing to significant improvement of the catalyst lifetime. This work demonstrated the potential applications of hollow hierarchical microsphere structure in catalytic engineering.

### 1. Introduction

In the past decade, inorganic hollow spheres from nanometer to micrometer dimensions have received increasing interest because of their unique physicochemical properties such as their distinct low effective density and

high specific surface area, which may open new possibilities in controlled storage and release, adsorption, catalysis, acoustic insulation, piezoelectric transducers, optics, sensors, and manufacture of advanced materials.<sup>1–6</sup> Caruso provided short reviews about hollow spheres and focused on a recent novel and versatile technique, based on a combination of colloidal templating and self-assembly processes, which could readily afford control over the size, composition, and wall thickness of the hollow spheres.<sup>1c,d</sup> To date, hollow spheres of various compositions such as oxide,<sup>2</sup> metal,<sup>3</sup> sulfide,<sup>4</sup> and carbon<sup>5</sup> have been produced. Taking into account the greatly different properties of various inorganic compounds that would benefit specific applications, the development of fabrication strategy and the construction of special functions for hollow structures built from various inorganic compositions is of both scientific and technological significance.

More recently, hollow spheres with a shell of material zeolites attract great attentions.<sup>6</sup> Zeolites are a class of microporous crystalline materials with pores of molecular dimensions widely used in industry as adsorbents,

\*Corresponding author. Tel.: +86 411 3989 3632. Fax: +86 411 8365 3220.  
E-mail: yjianhua@dlut.edu.cn.

- (1) (a) Caruso, F.; Caruso, R. A.; Möhwald, H. *Science* **1998**, *282*, 1111. (b) Schärfl, W. *Adv. Mater.* **2000**, *12*, 1899. (c) Caruso, F. *Chem.—Eur. J.* **2000**, *6*, 413. (d) Caruso, F. *Adv. Mater.* **2001**, *13*, 11. (e) Yang, Z.; Niu, Z.; Lu, Y.; Hu, Z.; Han, C. C. *Angew. Chem., Int. Ed.* **2003**, *42*, 1943. (f) Yin, Y.; Rioux, R. M.; Erdonmez, C. K.; Hughes, S.; Somorjai, G. A.; Paul Alivisatos, A. *Science* **2004**, *304*, 711.
- (2) (a) Iida, M.; Sasaki, T.; Watanabe, M. *Chem. Mater.* **1998**, *10*, 3780. (b) Caruso, F.; Caruso, R. A.; Möhwald, H. *Chem. Mater.* **1999**, *11*, 3309. (c) Niu, Z.; Yang, Z.; Hu, Z.; Lu, Y.; Han, C. C. *Adv. Funct. Mater.* **2003**, *13*, 949. (d) Cao, M.; Hu, J.; Liang, H.; Wan, L. *Angew. Chem., Int. Ed.* **2005**, *44*, 4391. (e) Wang, W.; Zhu, Y.; Yang, L. *Adv. Funct. Mater.* **2007**, *17*, 59. (f) Cong, H.; Yu, S. *Adv. Funct. Mater.* **2007**, *17*, 1814. (g) Chen, D.; Ye, J. *Adv. Funct. Mater.* **2008**, *18*, 1922. (h) Zhao, W.; Chen, H.; Li, Y.; Li, L.; Li, M.; Shi, J. *Adv. Funct. Mater.* **2008**, *18*, 2780.
- (3) (a) Marinakos, S. M.; Novak, J. P.; Brousseau, L. C., III; House, A. B.; Edeki, E. M.; Feldhaus, J. C.; Feldheim, D. L. *J. Am. Chem. Soc.* **1999**, *121*, 8518. (b) Liang, Z.; Susha, A.; Caruso, F. *Chem. Mater.* **2003**, *15*, 3176. (c) Peng, Q.; Dong, Y.; Li, Y. *Angew. Chem., Int. Ed.* **2003**, *42*, 3027. (d) Arnal, P. M.; Comotti, M.; Schüth, F. *Angew. Chem., Int. Ed.* **2006**, *45*, 8224.
- (4) (a) Hu, Y.; Chen, J.; Chen, W.; Li, X. *Adv. Funct. Mater.* **2004**, *14*, 383. (b) Cao, X.; Gu, L.; Zhuge, L.; Gao, W.; Wang, W.; Wu, S. *Adv. Funct. Mater.* **2006**, *16*, 896. (c) Yu, X.; Cao, C.; Zhu, H.; Li, Q.; Liu, C.; Gong, Q. *Adv. Funct. Mater.* **2007**, *17*, 1397.
- (5) (a) Gierszal, K. P.; Jaroniec, M. *J. Am. Chem. Soc.* **2006**, *128*, 10026. (b) Ikeda, S.; Ishino, S.; Harada, T.; Okamoto, N.; Sakata, T.; Mori, H.; Kuwadata, S.; Torimoto, T.; Matsumura, M. *Angew. Chem., Int. Ed.* **2006**, *45*, 7063. (c) Titirici, M. M.; Thomas, A.; Antonietti, M. *Adv. Funct. Mater.* **2007**, *17*, 1010. (d) Tao, Y.; Endo, M.; Kaneko, K. *J. Am. Chem. Soc.* **2009**, *131*, 904.

- (6) (a) Wang, X.; Yang, W.; Tang, Y.; Wang, Y.; Fu, S.; Gao, Z. *Chem. Commun.* **2000**, 2161. (b) Valtchev, V.; Mintova, S. *Micro. Meso. Mater.* **2001**, *43*, 41. (c) Valtchev, V. *Chem. Mater.* **2002**, *14*, 956. (d) Dong, A.; Wang, Y.; Tang, Y.; Ren, N.; Zhang, Y.; Gao, Z. *Chem. Mater.* **2002**, *14*, 3217. (e) Valtchev, V. *Chem. Mater.* **2002**, *14*, 4371. (f) Dong, A.; Ren, N.; Yang, W.; Wang, Y.; Zhang, Y.; Wang, D.; Hu, J.; Gao, Z.; Tang, Y. *Adv. Funct. Mater.* **2003**, *13*, 943. (g) Naik, S. P.; Chiang, A. S. T.; Thompson, R. W.; Huang, F. C. *Chem. Mater.* **2003**, *15*, 787. (h) Xiong, C.; Coutinho, D.; Balkus, K. J., Jr. *Microporous Mesoporous Mater.* **2005**, *86*, 14.

ion exchangers, separation membranes, and in particular as solid acid catalysts in the fields of oil refining and petrochemistry.<sup>7</sup> It is indisputable that hollow zeolite microspheres represent for a special group of hollow structural materials in view of the high thermal and chemical stability as well as intrinsic scientific interest in their diverse chemistry. Because a layer-by-layer (LbL) technique based on electrostatic interaction or hydrogen bonding was reported by Caruso,<sup>1a</sup> there have been several reports on the syntheses of hollow zeolite microspheres using polystyrene spheres (PS) as templates and applying LbL or secondary growth synthesis approaches. Tang et al. reported the fabrication of hollow zeolite (silicalite-1 and  $\beta$ ) spheres through an LbL technique using PS as templates and nanozeolites as building blocks, followed by calcination.<sup>6a</sup> Subsequently, Valtchev introduced a combination of LbL and hydrothermal synthesis techniques to prepare core-shell polystyrene/zeolite A microbeads<sup>6c</sup> and silicalite-1 hollow spheres and bodies with a regular system of macrocavities.<sup>6e</sup> In this way, the zeolite shells are built of well-intergrown crystals so as to improve the mechanical stability and intact ratio of the obtained hollow spheres. Nevertheless, these methods for the hollow zeolite microspheres relied on generated beforehand building block of nanozeolite particles and the LbL technique in which the necessary multistep alternatively coating processes are rather complicated and labor intensive. More importantly, there was lack of application of hollow zeolites reported to date, although new application and unique properties are highly expected for them either in traditional use areas or advanced areas.

Zeolite MCM-22 is a microporous materials composed of interconnected building units that form two independent pore systems: two-dimensional 10-ring sinusoidal channels, and 12-ring interlayer supercages with depths of 18.2 Å, both of which are accessible through 10-ring apertures.<sup>8</sup> This makes MCM-22 a promising catalyst for many processes, particularly for methane dehydroaromatization reaction (MDA),<sup>9</sup> which provides alternative route to petroleum for the production of benzene and become an important branch of C1 chemistry. Herein, we report the synthesis of hollow hierarchical MCM-22 microspheres (simplified as MCM-22-HS) by a facile one-pot hydrothermal method involving self-assembly combined hydrothermal synthesis with carbon black spheres as core-template. To the best of our knowledge, synthesis of zeolite hollow spheres by such carbon tem-

plating method has not been reported to date. Furthermore, the exceptional catalytic performance in MDA reaction related to the hollow hierarchical MCM-22 structure was demonstrated.

## 2. Experimental Section

**2.1. Synthesis.** All chemical reagents used in this work were of analytical grade. The MCM-22-HS was synthesized using hexamethyleneimine (HMI) as a structure direction agent (SDA) and carbon black microspheres as hard core template. The used carbon black microspheres (M700, purchased from Cabot Corporation) with particle diameter 4–8  $\mu\text{m}$  possesses BET surface area of 257  $\text{m}^2/\text{g}$  with pore size ranging from 20 to 30 nm. Known amounts of sodium metaaluminate ( $\text{NaAlO}_2$ , supplied by Tianjin Bodi Chemical Co., Ltd.), sodium hydroxide (96% NaOH, supplied by Tianjin Bodi Chemical Co., Ltd.), HMI (>99%, purchased from Aldrich) and deionized water (supplied by DLUT) were mixed and vigorously agitated in a vessel for 30 min. Subsequently, a specific amount carbon black microspheres, which were dried in an oven (393 K) overnight, was impregnated with this solution and vigorously agitated for 6 h. The weight ratio between the Al-containing precursor solution and the carbon black impregnated is about 10. Ludox (AS-40, 40%  $\text{SiO}_2$ , Aldrich) was then added into the mixture by dropping with one drop per two seconds. The molar composition of the final mixture was as follow:  $\text{Al}_2\text{O}_3\cdot 30\text{SiO}_2\cdot 3\text{Na}_2\text{O}\cdot 1500\text{H}_2\text{O}\cdot 15\text{HMI}$ . The resultant mixture of 80 mL was introduced into a stainless-steel autoclave (100 mL), followed by heating to 423 K for 7 days under the condition of rotating crystallization. After quenching the autoclave to room temperature, the solid sample was separated from the mixture by centrifugation (5000 r/min), washed by deionized water then dried at 393 K overnight. The SDA and the carbon black microspheres were removed by controlled calcination in air in a muffle at 823 K for 12 h at a heating and cooling rate of 0.5 and 0.9 K/min, respectively. In this way, a white material (MCM-22-HS) is obtained. For comparison, the synthesis experiment was carried out with the synthesis parameters kept as same as that of MCM-22-HS except for the presence of carbon black template so as to obtained conventional flaky MCM-22 zeolites.

H-form MCM-22-HS and MCM-22 zeolites were obtained by successive exchanging with 1 M  $\text{NH}_4\text{NO}_3$  aqueous solution and calcination. Then, Mo-containing catalysts (Mo wt% = 6%) were prepared by incipient wetness impregnation of the obtained MCM-22-HS and MCM-22 with an aqueous solution of ammonium molybdate according to the procedure as precisely described in the previous studies<sup>9</sup> and denoted as Mo/HMCM-22-HS and Mo/HMCM-22 catalysts, respectively. After impregnation, the catalysts were dried at 393 K for 4 h and then calcined in air at 773 K for 6 h as described in the previous studies.<sup>9</sup> Besides, all the conditions for the two catalysts preparation were kept same for comparison.

**2.2. Catalyst Evaluation.** The MDA reaction was carried out in a quartz tubular fixed-bed reactor (8 mm i.d.) at atmospheric pressure and 973 K, a space velocity of 1500 mL/(g h). The products were analyzed by an online gas chromatograph equipped with ten-way sampling valve (Valco) for autosampling every time per 30 min, a flame ionization detector (FID) for the analysis of  $\text{CH}_4$ ,  $\text{C}_6\text{H}_6$ ,  $\text{C}_7\text{H}_8$ , and  $\text{C}_{10}\text{H}_8$ , and a thermal conductivity detector (TCD) for the analysis of  $\text{H}_2$ ,  $\text{N}_2$ ,  $\text{CH}_4$ ,  $\text{CO}$ ,  $\text{C}_2\text{H}_4$ , and  $\text{C}_2\text{H}_6$ . The feed was a gas mixture of 10%  $\text{N}_2/\text{CH}_4$  and the  $\text{N}_2$  in the feed was used as an internal standard for

- (7) (a) Jacobs, P. A.; Martens, J. A. *Stud. Surf. Sci. Catal.* **1991**, *58*, 445. (b) Corma, A. *Chem. Rev.* **1995**, *95*, 559. (c) Corma, A. *Chem. Rev.* **1997**, *97*, 2373. (d) Davis, M. E. *Nature* **2002**, *417*, 813. (e) Cundy, C. S.; Cox, P. A. *Chem. Rev.* **2003**, *103*, 663. (f) Tosheva, L.; Valtchev, V. P. *Chem. Mater.* **2005**, *17*, 2494.
- (8) (a) Chu, C. T. W. US Patent 4 956 514 1990; (b) Corma, A.; Corell, C.; Lopic, F.; Martinez, A.; Perez-Pariente, J. *Appl. Catal., A* **1994**, *115*, 121. (c) Lawton, J. A.; Lawton, S. L.; Leonowicz, M. E.; Rubin, M. K. *Stud. Surf. Sci. Catal.* **1995**, *98*, 250. (d) Corma, A.; Corell, C.; Perez-Pariente, J. *Zeolites* **1995**, *15*, 2. (e) Corma, A.; Martinez-Soria, V.; Schnoefeld, E. *J. Catal.* **2000**, *192*, 163.
- (9) (a) Shu, Y.; Ma, D.; Xu, L.; Xu, Y.; Bao, X. *Catal. Lett.* **2000**, *70*, 67. (b) Liu, L.; Ma, D.; Chen, H.; Zheng, H.; Cheng, M.; Xu, Y.; Bao, X. *Catal. Lett.* **2006**, *108*, 25.

analyzing all products, including carbonaceous deposition on the basis of converted methane molecules.

**2.3. Characterization.** The synthesized products were characterized by X-ray powder diffraction (XRD) on a Rigaku-Dmax 2400 diffractometer equipped with graphite monochromatized CuK $\alpha$  radiation in the  $2\theta$  angle ranging from 0.5 to 50°, scanning electron micrograph (SEM, KYKY-2800B). Transmission electron microscopy (TEM) was carried out on a Philips Tecnai G2 20 instrument, operating at 200 kV. Nitrogen adsorption analyses was carried out with an Autosorb-1 adsorption analyzer (Quantachrome Instruments) at 77 K. Prior to the adsorption measurements, the sample was degassed at 473 K for at least 6 h. Pore size distribution was obtained by BJH method. The X-ray fluorescence (XRF) spectrometry analysis was carried on Bruck SXR SKS-3400 instrument. For the NH<sub>3</sub>-TPD experiments, the sample (0.14 g) was dried in a flowing He (99.99%, 30 mL/min) at 873 K for 0.5 h prior to adsorption. Pure NH<sub>3</sub> was adsorbed until saturation took place at 323 K, then the catalyst was flushed with He at the same temperature for 1 h. TPD measurements were conducted from 323 to 900 K with a heating rate of 15 K, with He as carrier gas. The amount of desorbed ammonia was detected by a thermal conductive detector.

### 3. Results and Discussion

**3.1. Preparation of MCM-22-HS.** XRD patterns (Figure 1) of the calcined products showed well-resolved peaks in the 4–40° range characteristic for MCM-22 structure<sup>10</sup> without the presence of peaks of other crystalline phases and amorphous phase, confirming the formation of MCM-22 zeolite with the high crystallinity.

The formation of the hierarchical hollow MCM-22 microspheric structure was revealed by SEM and TEM images of the products in Figure 2. The SEM images in Figure 2a, b showed beautiful nestlike microspheres that were constructed compactly by many flaky crystals. Such unusual spherical architecture is entirely distinct from the typical flaky morphology of the MCM-22 zeolite in Figure 3 synthesized with the same synthesis compositions and procedures as MCM-22-HS without adding carbon black particles. More detailed structural features of the spherical architecture were revealed by SEM image of a few individual microspheres with collapse-fissure (Figure 2c), clearly exhibiting that the individual microsphere was hollow and the thickness of the shell was quite uniform. TEM images (Figure 2d) further revealed the hollow structure and the stacking of the building units of MCM-22 nanocrystals (as shown in the insert) since the contrast at the center was much lower than that of a solid particle. Besides, clear lattice fringes were observed, revealing the high crystallinity of this sample. It is worth noting that most of the products (>85%) present the intact spherical morphology similar to that of the carbon black particles (see the Supporting Information, Figure 1), suggesting the good mechanical strength of the products.

N<sub>2</sub> adsorption isotherm (Figure 4) of the MCM-22-HS showed a clear hysteresis loop at about relative pressure

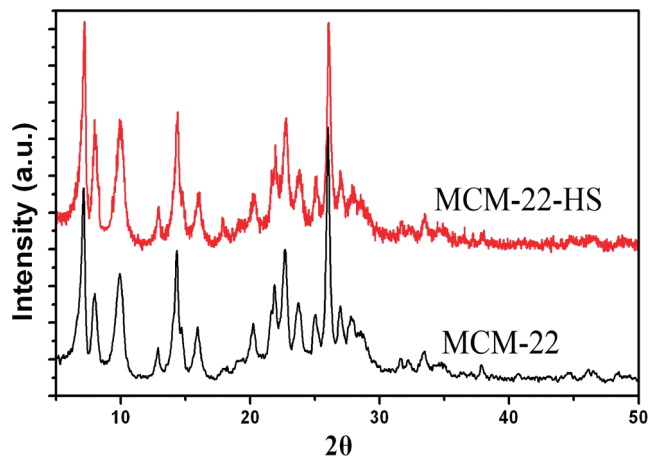


**Figure 1.** Wide-angle XRD patterns of the calcined products using carbon black as core template and the typical flaky MCM-22 zeolite synthesized in this work with the same synthesis compositions and procedures as MCM-22-HS without adding carbon black particles.

$P/P_0$  0.5–0.98, caused by the capillary condensation in the textural mesopores, indicating the presence of mesopores that were reasonably assigned to intercrystalline voids between the flaky nanocrystals. The mesoporous structure in microporous zeolites is particularly important for practical application of zeolite.<sup>11</sup> The BJH average pore diameter of the sample is about 16.1 nm based on the desorption branch of the isotherm. The BET surface area and micropore area of MCM-22-HS is 471 and 337 m<sup>2</sup>/g, respectively. Compared with the conventional typical flake MCM-22 with BET surface area and micropore area of 458 and 352 m<sup>2</sup>/g, respectively, it possessed a higher external surface area of 134 m<sup>2</sup>/g and lower micropore surface area of 337 m<sup>2</sup>/g (see the Supporting Information, Table 1). The above observations revealed the formation of the hierarchical and hollow MCM-22 microsphere via carbon black templating hydrothermal synthesis.

**3.2. Growth Mechanism.** Time trial study of the growth process aided us in understanding the formation mechanism of the hollow hierarchical structure. TEM images and XRD patterns of the calcined products at different growth periods is shown in Figure 5. Judging from the low contrast in the TEM images (Figure 5a, b) and amorphous XRD patterns in (Figure 5e), the hollow microspheres with amorphous shell were formed in the first 4 days. Increasing the crystallization time yielded crystalline phase for the shell but did not affect the hollow structure. The shell showed the emergence of the crystalline MCM-22 structure after 6 days (Figure 5c, e). The microspheres with the shell consisting of highly crystalline and intergrown MCM-22 crystals were obtained after 7 days (Figure 5d, e).

- (11) (a) Tao, Y. S.; Kanoh, H.; Kaneko, K. *J. Am. Chem. Soc.* **2003**, *125*, 6044. (b) Kustova, M. Y.; Hasselriis, P.; Christensen, C. H. *Catal. Lett.* **2004**, *96*, 205. (c) Christensen, C. H.; Schmidt, I.; Carlsson, A.; Johannsen, K.; Herbst, K. *J. Am. Chem. Soc.* **2005**, *127*, 8098. (d) Schüth, F. *Annu. Rev. Mater. Res.* **2005**, *35*, 209. (e) Li, W. C.; Lu, A. H.; Palkovits, R.; Schmidt, W.; Spliethoff, B.; Schüth, F. *J. Am. Chem. Soc.* **2005**, *127*, 12595.

(10) Corma, A.; Corell, C.; Perez-Pariente, J. *Zeolites* **1995**, *15*, 2.

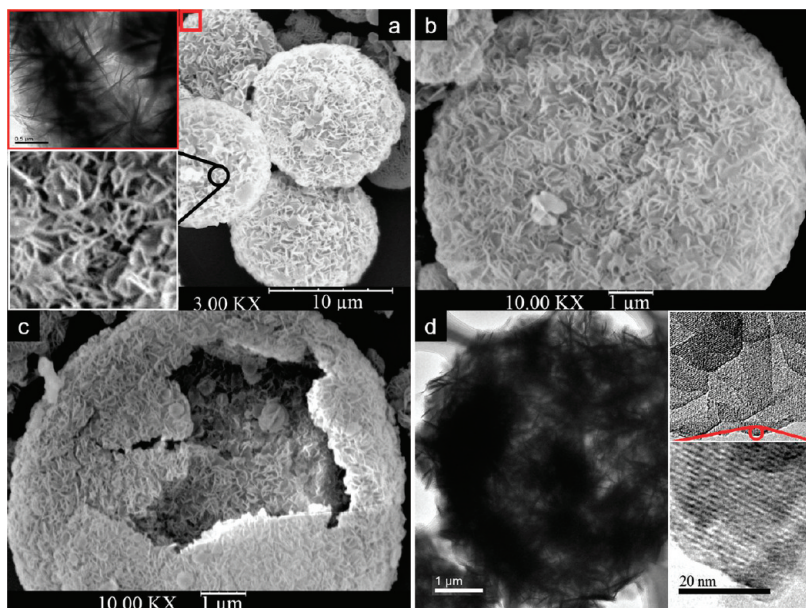


**Figure 2.** SEM images of (a, b) the sample synthesized in this work and (c) the sample with collapse-fissure; (d) TEM images of the calcined sample; inset, high-resolution TEM image of the area marked by red circle.

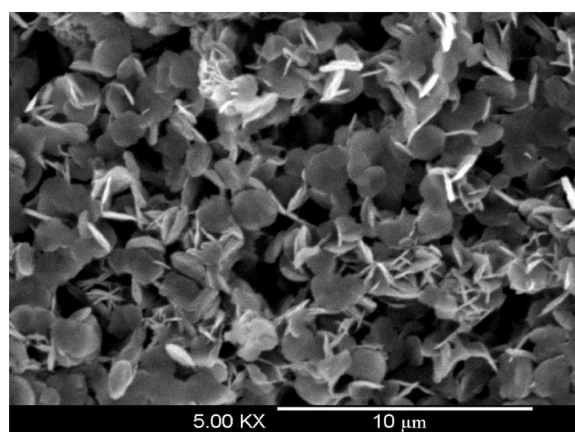


**Figure 3.** SEM image of typical flaky MCM-22 zeolite synthesized with the same synthesis compositions and procedures as MCM-22-HS without adding carbon black particles.

A clearer description of the formation process is illustrated in Figure 6. In a typical synthesis procedure for MCM-22, the precursor particles reasonably containing silica and hydrophobic SDA<sup>12</sup> evolve into MCM-22 zeolites. When carbon black was added into the precursor solution, the precursor particles were assembled onto the external surface of the carbon black grains to form carbon@precursor particles core-shell structure. Carbon black particles are known to exhibit measurable amounts of polar surface chemical groups COH and COOH that will definitely interact with polar species also the alkanes.<sup>13</sup> IR spectrum (see the Supporting Information, Figure 2) confirmed the presence of the groups. The strong interactions of hydrogen bond between surface

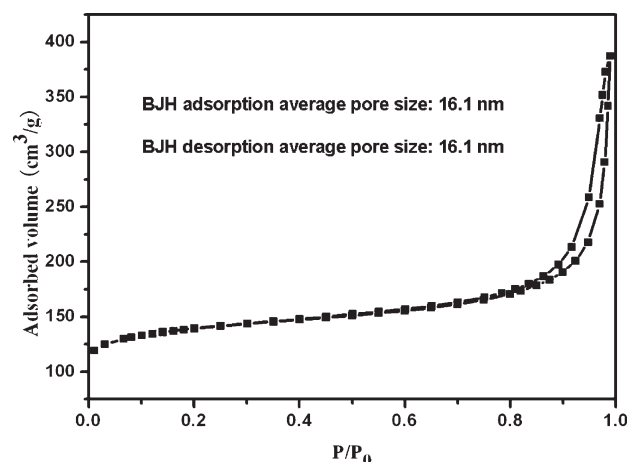


**Figure 4.** N<sub>2</sub> adsorption and desorption isotherms for obtained MCM-22-HS.

**Table 1. Catalytic Performance of Various Catalysts Being Subjected to MDA Reaction for a Certain Times (Mo-Based MCM-22 and ZSM-5 Catalysts for 24 and 10 h, Respectively)**

catalyst	$T^a$ (K)	benzene yield (%) <sup>b</sup>	benzene yield (%) <sup>c</sup>	ref
Mo/HMCM-22	973	8	6.1	<sup>9</sup>
Mo/HMCM-22	973	6.8	4.7	this work
Mo/HMCM-22-HS	973	9.3	9.08	this work
Mo/HZSM5-P <sup>d</sup>	973	8.5	5.4	<sup>16b</sup>
Mo/HZSM5-ST <sup>2c</sup>	973	9.4	7.2	<sup>16b</sup>

<sup>a</sup> The thermodynamic equilibrium conversion of CH<sub>4</sub> for CH<sub>4</sub> reaction to benzene is 11.5% at 973 K.  $6\text{CH}_4 \rightarrow \text{C}_6\text{H}_6 + 9\text{H}_2$ ;  $\Delta H_f = -530$  kJ/mol. <sup>b</sup> The highest yield of benzene and the lowest yield of benzene. <sup>c</sup> During the decline curve. <sup>d</sup> The parent zeolite catalyst used in ref 16b. <sup>e</sup> The catalyst after dealumination treatment of the parent zeolite catalyst under the conditions of 823 K, partial pressure of steam of 38 kPa, and for 6 h.

- (12) Lawton, S. L.; Fung, A. S.; Kennedy, G. J.; Alemany, L. B.; Chang, C. D.; Hatzikos, G. H.; Lissy, D. N.; Rubin, M. K.; Timken, H. C.; Steuernagel, S.; Woessner, D. E. *J. Phys. Chem.* **1996**, *100*, 3788.  
 (13) (a) Papirer, E.; Brendle, E.; Ozil, F.; Balard, H. *Carbon* **1999**, *37*, 1265. (b) Lin, J. H. *Carbon* **2002**, *40*, 183.

groups of carbon black particles and the plenty of OH groups, Si-O, Al-O bonds, and the NH group in the precursor particles probably is the driving force of the

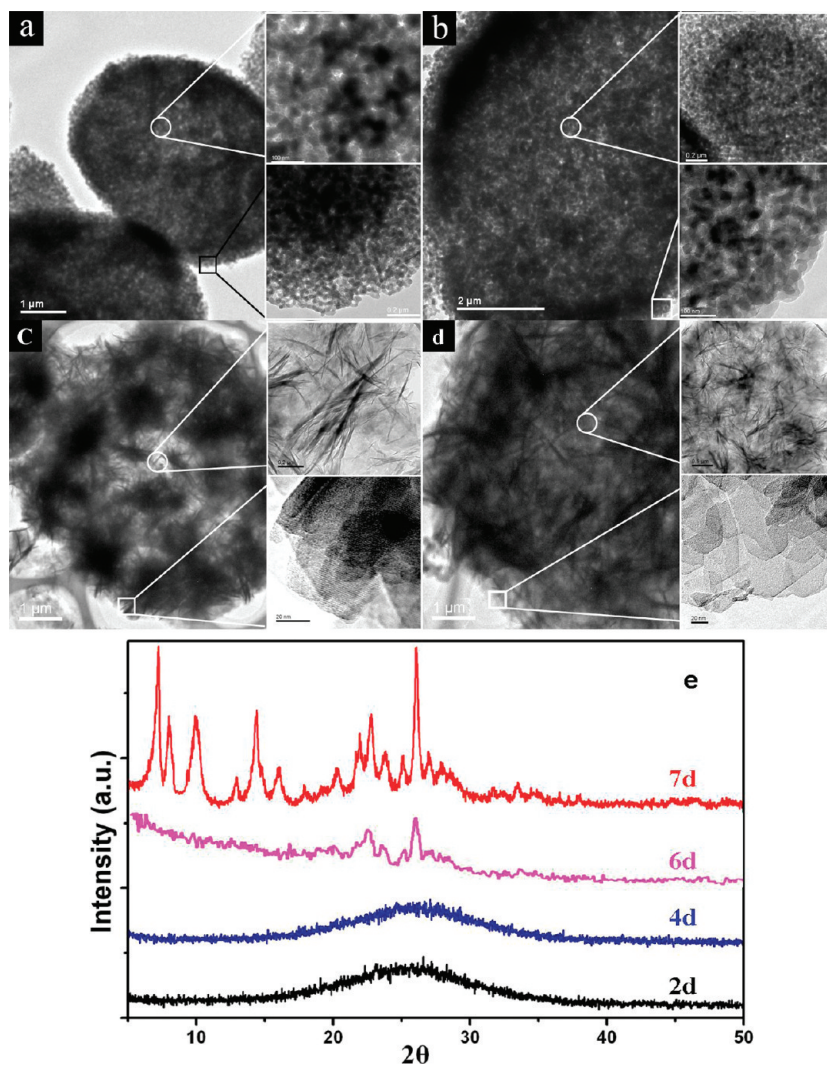


**Figure 5.** TEM images of calcined products at different growth periods: (a) 2 days; (b) 4 days; (c) 6 days; (d) 7 days; and (e) the wide-angle XRD patterns of the calcined products at different growth periods (2, 4, 6, and 7 days).

assembly of precursor nanoprecursor particles onto the carbon black particles. Nevertheless, the rotating condition was the prerequisite that could ensure the homogeneous dispersion of carbon black microspheres in the synthesis mixture and the necessary contact of the precursor gels with carbon black microspheres. The precursor particles assembled onto the surface of carbon black grains then nucleated and crystallized to yield carbon@polycrystalline MCM-22 core-shell structure with the elapsed reaction time. By calcination, the HMI structure-directing agent and carbon core template were removed, forming hollow MCM-22 structure.

**3.3. Catalyst Performance Evaluation.** Methane dehydroaromatization (MDA) reaction being considered as a promising route for direct conversion of methane into high value-added chemicals has attracted increasing attentions in the past several decades. Although remarkable progress has been made in this field in terms of catalyst, many important features and findings discovered,<sup>14</sup> MDA remains an important industrial challenge

because of severely thermodynamically limited conversion and intractable carbon deposition resulting in severe catalysis deactivation. To evaluate the properties of the MCM-22-HS, the MDA as a model reaction was tested over Mo/HMCM-22-HS catalyst. Mo content of 6 wt % was chosen for both Mo/HMCM-22-HS and the traditional Mo/HMCM-22 catalysts, which was reported to be the optimized content for Mo/HMCM-22.<sup>9</sup> Besides, To compare the catalytic performances of these two catalysts, we prepared both the Mo/HMCM-22 and Mo/HMCM-22-HS catalysts using the same procedures and operated the MDA conversion under the same reaction conditions, such as the same weights of the zeolite supports and Mo contents for these two kinds of catalysts, reaction temperature, space velocity. The XRF analysis of the two catalysts (not shown here) shows that calcined Mo/HMCM-22-HS catalyst possesses the similarity to the calcined Mo/HMCM-22 catalyst in terms of Mo content (6.0 and 5.9 wt %, respectively) and Si/Al ratio.

Figure 7a presents methane conversion and the distribution of products being benzene, naphthalene, carbon deposition (the very trace of ethane and CO is included

(14) (a) Xu, Y.; Lin, L. *Appl. Catal., A* **1999**, *188*, 53. (b) Xu, Y.; Bao, X.; Lin, L. *J. Catal.* **2003**, *216*, 386.

into carbon deposition) for Mo/HMCM-22-HS together with the conventional flaky Mo/HMCM-22 prepared in the present work (Figure 3). Our conventional Mo/HMCM-22 catalyst presented a comparable catalytic performance with that of Mo/HMCM-22 reported by Bao<sup>9</sup> which is found the best catalyst for MDA. Astonishingly, the MCM-22-HS catalyst exhibited remarkably high CH<sub>4</sub> conversion and high yield of benzene increased by 25–30% relative to that of the conventional Mo/HMCM-22 catalysts either synthesized in the present work or reported by Bao. The yield of carbon deposition was much higher than that of the conventional one, whereas the Mo/HMCM-22-HS catalyst displayed exceptional catalyst stability with the benzene yield of 9% keeping almost constant until the reaction runs for 3000 min. Under the same reaction conditions employed, formation rates of benzene on these two catalysts were shown in Figure 7b. Clearly, the formation rate of benzene on the conventional Mo/HMCM-22 catalyst started to decline abruptly from 400 min of time-on-stream, implying the rapid deactivation of catalyst from 400 min. On the contrary, the formation rate of benzene on the Mo/HMCM-22-HS catalyst was quite constant after induction period and decline slightly during the

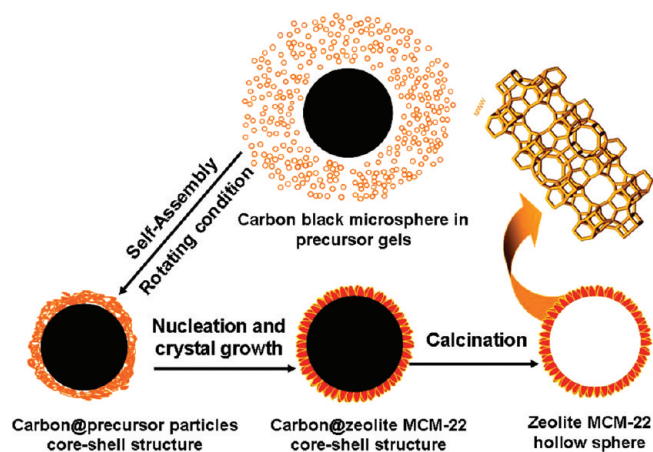
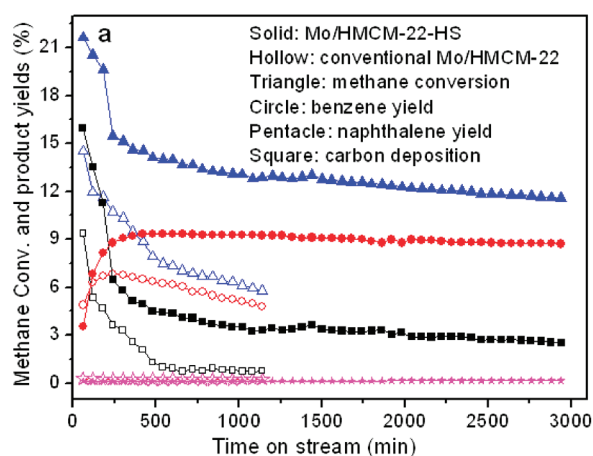


Figure 6. Schematic representation of the growth process of the MCM-22-HS.



whole time-on-stream (3000 min), indicating that the catalyst activity is quite stable. The comparison of the catalytic performance of the reported catalysts for MDA reaction at various moments including the steam dealuminated HZSM-5 supported molybdenum, which was reported to be highly coking resistant (Table 1) further displays the exceptional benzene yield and catalyst stability. To the best of our knowledge, among the reported catalysts for MDA reaction, the Mo/HMCM-22-HS catalyst showed the highest benzene yield and catalyst stability.

NH<sub>3</sub>-TPD analysis was conducted for the conventional HMCM-22 zeolite (1), calcined Mo/HMCM-22 catalyst (2), the HMCM-22-HS zeolite (3), and calcined Mo/HMCM-22-HS catalyst (4) as shown in the Supporting Information, Figure 3. Interestingly, the calcined Mo/HMCM-22-HS showed a much smaller peak area of high temperature (Peak H) that is assigned to the desorption of NH<sub>3</sub> adspecies adsorbed on exchangeable Brønsted acid sites<sup>9a</sup> in comparison with calcined Mo/HMCM-22 catalyst, although HMCM-22-HS zeolite showed a higher Peak H than HMCM-22 catalyst. In a word, the amount of Brønsted acid sites of HMCM-22-HS is much more reduced than that of HMCM-22 zeolite after Mo modification. It is recognized that the reduction in amount of Brønsted acid sites is due to the occupation of the MoO<sub>x</sub> species that exchange with Brønsted acid sites to form Mo–O–Al bond during the impregnation and calcinations.<sup>14</sup> Hence, it can be inferred that more exchanged Mo species that are evolved into MoC<sub>x</sub> or MoO<sub>x</sub>C<sub>y</sub> species being the active site of activation of methane were formed for Mo/HMCM-22-HS catalyst during the impregnation and calcination course. The more active sites naturally give rise to high methane conversion and thus high benzene yield. This deduction can be further supported by the observed high yield of carbonaceous deposition one components of which is reactive MoC<sub>x</sub> or MoO<sub>x</sub>C<sub>y</sub>.<sup>15</sup> It can be therefore concluded that the remarkably enhanced high conversion is attributed to the formation of more active sites for methane activation. It is well demonstrated that the hierarchical pore architecture

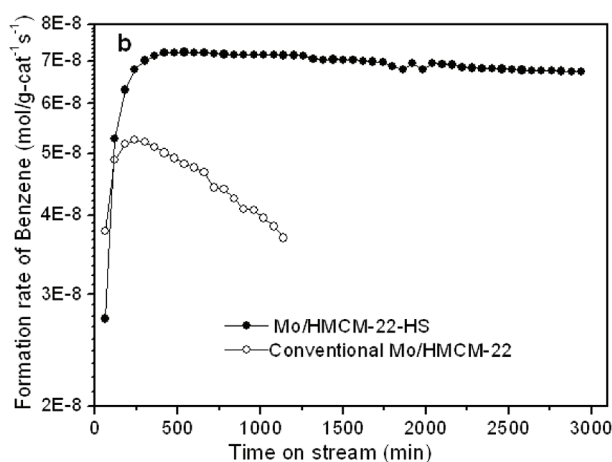


Figure 7. (a) Catalytic performances of Mo/HMCM-22-HS and conventional Mo/HMCM-22 catalysts for MDA reaction; (b) formation rates of benzene at 973 K on these two catalysts under space velocity of 1500 mL/(g h).

significantly improve mass transport limitation, resulting in improved activity for mesoporous zeolite catalyst.<sup>16</sup> In our case, the higher external surface of hierarchical MCM-22-HS shell probably leads to higher dispersion of Mo precursor species onto the MCM-22 external surface, which is the initial stage of the exchange of Mo species with MCM-22.<sup>15</sup> Furthermore, the presence of the mesopores leads to faster transfer of Mo species into the MCM-22 channels. All these are favorable for better migration of Mo species into MCM-22 zeolite channel, giving rise to more Mo species exchanged with acid sites of OH groups. Also, the more Brønsted acid sites in HMCM-22-HS zeolite are probably favorable for the exchange of MoO<sub>x</sub> species with them. The exact reason for the formation of more active sites for methane activation should be further investigated by using <sup>29</sup>Si MAS NMR, <sup>27</sup>Al MAS NMR, <sup>1</sup>H MAS NMR, and <sup>95</sup>Mo NMR, etc., techniques.

For the catalysis stability of MDA, it is recognized that the excess of Brønsted acid sites result in catalyst deactivation since Brønsted acid sites are not only responsible for the formation of aromatics products but also for the deposition of aromatic-type coke causing catalyst deactivation.<sup>15</sup> For the calcined Mo/MCM-22-HS catalyst, the retained Brønsted acid sites was indeed much less than that of the calcined Mo/HMCM-22 catalyst as shown in the Supporting Information Figure 3. The highly enhanced catalyst lifetime of Mo/MCM-22-HS could be therefore attributed to the less Brønsted acid sites due to the occupation of Brønsted acid sites by Mo species.<sup>17</sup> Moreover, hollow interior structure probably made the intercrystalline mesopores among the shell more active for access of larger product molecules like benzene because of the larger possibility for the mesopores mouth to direct open to the interior void, the fast transport of larger products nevertheless is in favor for improving the catalyst activity and lifetime as reported in literature work.<sup>16</sup>

The high benzene yield and long lifetime resulted from the hollow and hierarchical structure which functionally

facilitated the formation of more active center probably through the prompted distribution of the active species into reaction sites and the promoted diffusion of large molecule products off the reaction sites. The formation of more active center simultaneously reduced the number of sites resulting in catalyst deactivation. Hence, the excellent catalytic performance for Mo/HMCM-22-HS in MDA reaction elucidates the claimed hollow and hierarchical structure of MCM-22-HS. These results also show that the hollow hierarchical microstructure is important to high catalytic performance.

#### 4. Conclusions

An unusually hollow hierarchical MCM-22-HS was successfully fabricated by one-pot hydrothermal synthesis under rotating crystallization conditions using carbon black microspheres as hard template. The formation process of MCM-22-HS was involved self-assembly and hydrothermal crystallization process. The MCM-22-HS exhibited significantly enhanced benzene yield and catalyst lifetime in MDA reaction. It is believed that the exceptional catalyst performance is due to hierarchical and hollow structure. The mesopores resulting higher external surface and hollow structure offered an important effect on improving the high benzene yield and catalyst lifetime by generating more catalysis active sites via promoted catalyst transport onto the reaction sites and by improving diffusion of larger product through the zeolite catalyst, respectively. The sites associated with catalyst deactivation could also be reduced, contributing to improvement of the catalyst lifetime. A facile and effective method was demonstrated to synthesize zeolite hollow spheres. This work demonstrated the potential applications of hollow hierarchical microsphere structure in catalytic engineering. We believe this work opens a door for application of hollow zeolite spheres.

**Acknowledgment.** The authors are greatly thankful for the valuable help and discussions from Prof. Xinhe Bao, Prof. Ding Ma, and Prof. Yushan Yan. Financial support from the National Key Technology R&D Program (2006BAE02B05) and the National Natural Science Foundation of China (20606004) is greatly acknowledged.

**Supporting Information Available:** The relevant SEM, BET, NH<sub>3</sub>-TPD analysis of products obtained in this work, and FT-IR analysis of carbon black microsphere used in this work (PDF). This material is available free of charge via the Internet at <http://pubs.acs.org>.

- (15) (a) Liu, H.; Li, T.; Tian, B.; Xu, Y. *Appl. Catal., A* **2001**, *213*, 103. (b) Ma, D.; Lu, Y.; Su, L.; Xu, Z.; Tian, Z.; Xu, Y.; Lin, L.; Bao, X. *J. Phys. Chem. B* **2002**, *106*, 8524. (c) Ma, D.; Wang, D.; Su, L.; Shu, Y.; Xu, Y.; Bao, X. *J. Catal.* **2002**, *208*, 260. (d) Ding, W.; Meitzner, G. D.; Iglesia, E. *J. Catal.* **2002**, *206*, 14.
- (16) (a) Christensen, C. H.; Johannsen, K.; Schmidt, I.; Christensen, C. H. *J. Am. Chem. Soc.* **2003**, *125*, 13370. (b) Xiao, F. S.; Wang, L.; Yin, C.; Lin, K.; Di, Y.; Li, J.; Xu, R.; Su, D. S.; Schlgl, R.; Yokoi, T.; Tatsumi, T. *Angew. Chem., Int. Ed.* **2006**, *45*, 3090. (c) Egeblad, K.; Christensen, C. H.; Kustova, M.; Christensen, C. H. *Chem. Mater.* **2008**, *20*, 946.
- (17) (a) Wang, H.; Su, L.; Zhuang, J.; Tan, D.; Xu, Y.; Bao, X. *J. Phys. Chem. B* **2003**, *107*, 12964. (b) Song, Y.; Sun, C.; Shen, W.; Lin, L. *Appl. Catal., A* **2007**, *317*, 266.